

01,11

## Spinodal Decomposition of an Alloy with a Strong Concentration Dependence of the Mutual Diffusion Coefficient

© I.K. Razumov

M.N. Mikheev Institute of Metal Physics of Ural Branch of Russian Academy of Sciences,  
Yekaterinburg, Russia

E-mail: rik@imp.uran.ru

Received June 15, 2021

Revised June 15, 2021

Accepted September 9, 2021

It is shown that the kinetics of decomposition of an alloy with a strong concentration dependence of the mutual diffusion coefficient is qualitatively different from the widely known kinetics of spinodal decomposition, since it includes the formation of metastable (in the kinetic sense) precipitates of the intermediate composition. Concentration dependence of the mutual diffusion coefficient is particularly due to the difference in impurity diffusion coefficients, as well as component self-diffusion coefficients, and it increases as temperature decreases. The calculations use an expression for the flow of component atoms in the absence of the substance flow, obtained previously under the kinetic theory of vacancy diffusion („hole gas method“).

**Keywords:** spinodal decomposition, mutual diffusion coefficient, precipitates of intermediate composition.

DOI: 10.21883/PSS.2022.01.52483.143

### 1. Introduction

Spinodal decomposition (SD) in the phase transformation theory is the formation of concentration dissimilarities and subsequent lamination into phases due to chemical interaction of atoms in an initially homogeneous alloy [1,2]. The conventional SD kinetics includes the following stages: the wave stage (increase of long-wave composition fluctuations), coalescence of waves and evaporation-condensation of drops. The wave stage of decomposition was described for the first time in Cahn's papers [3,4]. The wave coalescence stage was studied, for instance, in papers [5,6]. Large precipitates at the evaporation-condensation stage grow due to the small ones, compliant with the Livshits–Slezov kinetics [7]. The alloy crystalline lattice during SD remains unchanged or rearranges at later stages.

Most papers pay special attention to the influence of thermodynamic factors (kind of the function of free-energy density, including the non-paired interatomic interactions or the possibility of ordering, long-range action, presence of gradient contributions in the functional of free energy, role of thermal fluctuations, cooling rate etc.) on the SD kinetics, while the diffusion coefficient is replaced by a constant for simplicity. In this case the characteristic diffusion length  $L = (D^*t)^{1/2}$  does not depend on coordinates, therefore a local thermodynamic equilibrium is quickly achieved at the boundary of the precipitate, and concentration in the volume of the growing precipitate approaches the equilibrium value. However, a change in the transformation kinematics should be anticipated if diffusion coefficients in the base and in the region of the forming precipitate differ significantly, since the precipitate in this case may grow in

conditions without an attained local equilibrium on its boundary.

It is known from the diffusion theory [1] that the rate of atom redistribution in a binary alloy is controlled by the mutual diffusion coefficient  $D = D_A^*c_A + D_B^*c_B$ , where  $D_{A(B)}^*$  are own (partial) diffusion coefficients,  $c_{A(B)}$  is the atomic concentration of components. Thereat, own diffusion coefficients are often considered to be close to diffusion coefficients of labelled atoms  $D_{A(B)}$ , which in general is not quite reasonable. Indeed, in the absence of substance flow (vacancy flow), it follows from the diffusion theory that  $D = D_A^* = D_B^*$  [1]. This condition can be physically assured by prohibiting the substance flow, e.g., by placing the alloy in a vessel with fixed walls. Since diffusion coefficients of labelled atoms  $D_{A(B)}$  are unchanged microscopic parameters, it follows that  $D_{A(B)} \neq D_{A(B)}^*$ . That's why the expression  $D \approx D_Ac_A + D_Bc_B$  can hold true only when substance flow is permitted (the Kirkendall effect [8]). In its turn, substance flows means the presence of sources and drains of nonequilibrium vacancies in the diffusion zone, which can be various lattice defects [9]. This situation is most typical in case of diffusion mixing of well-mixable metals brought into contact, and is less expected at the initial stages of spinodal decomposition from the homogeneous state.

Papers [10–12] within the framework of the kinetic theory of vacancy diffusion („hole gas method“ [13]) have obtained expressions for atom flows when vacancy concentration gradients are present. In this approach, if the vacancy flow is negligible ( $|J_V| \ll |J_{A(B)}|$ ), the vacancy subsystem reaches local equilibrium that corresponds to local concentrations of components, while the expression for the mutual diffusion coefficient is as follows:

Values of impurity diffusion and self-diffusion coefficients for some binary alloys based on reference data [15]

Alloy AB	$T, K$	$D_A(c_A \rightarrow 0),$ $m^2/s$	$D_B(c_B \rightarrow 0),$ $m^2/s$	$D_A(c_A = 1),$ $m^2/s$	$D_B(c_B = 1),$ $m^2/s$
FCC–FeCu	1200	$5 \cdot 10^{-14}$	$2.5 \cdot 10^{-17}$	$1.2 \cdot 10^{-17}$	$5.5 \cdot 10^{-14}$
FCC–AgCu	500	$2.5 \cdot 10^{-25}$	$2.1 \cdot 10^{-23}$	$7.3 \cdot 10^{-24}$	$1.8 \cdot 10^{-26}$
BCC–FeCr	750	$3.4 \cdot 10^{-28}$	$8.7 \cdot 10^{-22}$	$2.9 \cdot 10^{-22}$	$2 \cdot 10^{-32}$

$D = D_A D_B (1 - \Psi_{CACB}) / (D_{ACA} + D_{BCB})$ , and in the case of an ideal solid solution  $\Psi = 0$ . An essentially similar expression was obtained in paper [14]. It can be seen that the mutual diffusion coefficient in the limit cases of highly diluted solid solutions takes on values  $D = D_A(c_A \rightarrow 0)$  or  $D = D_B(c_B \rightarrow 0)$  respectively (hereinafter for brevity  $D_A(c_A \rightarrow 0) \equiv D_A^0$ ,  $D_B(c_B \rightarrow 0) \equiv D_B^0$ ). Consequently, regions evolve during SD where the mutual diffusion coefficient (and, together with it, own diffusion coefficients  $D_A^*, D_B^*$ ) varies from values close to  $D_A^0$  (impurity diffusion coefficient A in base B) to values close to  $D_B^0$  (impurity diffusion coefficient B in base A).

The table gives values of impurity diffusion coefficients  $D_A^0, D_B^0$ , as well as self-diffusion coefficients  $D_A^1, D_B^1$  for several alloys that undergo SD, based on the reference data [15]. It can be seen that the values of  $D_A^0, D_B^0$ , at the chosen temperatures differ by several orders. Thereat, the impurity diffusion coefficient in the base usually has a value of the same order as the self-diffusion coefficient for the base atoms. Since temperature dependencies of diffusion coefficients obey the Arrhenius law, the  $D_A/D_B$  ratio shall change exponentially as temperature decreases. SD is implemented in all the chosen cases without crystalline lattice rearrangement. Possible lattice rearrangement in other alloys during SD provides additional possibilities for the dependence of  $D$  on alloy's local state in the course of transformation.

The given data makes it possible to assume that precipitates during SD may quite probably grow in conditions far from a local equilibrium near the interphase boundary. Then a simple model is suggested for studying the SD kinetics with presence of a concentration dependence of the mutual diffusion coefficient  $D$ , and the typical scenarios obtained by numeric solving of the suggested equations are discussed.

## 2. Formulation of the model

According to [10,11,12], an expression for the atom flow of the component A in a binary alloy with prohibited substance flow (i.e. within the small vacancy flow,  $|J_V| \ll |J_{A(B)}|$ ) can be written as

$$\mathbf{J}_A = -\frac{D_A D_B}{D_{ACA} + D_{BCB}} \left[ (1 - \Psi_{CACB}) \nabla c_A - R^2 \Psi_{CACB} \nabla \Delta c_A \right], \quad (1)$$

where  $D_i = c_V \omega_i$  — diffusion coefficients for labeled atoms,  $c_V$  — vacancy concentration,  $\omega_i$  — diffusion mobilities,

$c_{A(B)}$  — atomic concentrations of components linked by the condition  $c_A + c_B = 1$ ,  $\Psi = -2v/(kT)$  — dimensionless mixing energy,  $R$  — small parameter that determines the interphase boundary width. Diffusion coefficients  $D_i$  follow the Arrhenius equation where activation energy linearly depends on component concentration

$$D_i = D_{0i}^0 \exp \left[ -\frac{U_0 + U_1 c_i}{kT} \right]. \quad (2)$$

Given the fact that impurity diffusion coefficients  $D_i(c_i \rightarrow 0) \equiv D_i^0$  and self-diffusion coefficients  $D_i(c_i = 1) \equiv D_i^1$  are known from experiments, let us rewrite (2) in the equivalent form

$$D_i = D_i^0 [D_i^1 / D_i^0]^{c_i}. \quad (3)$$

The evolution of the alloy is described by the continuity equation

$$\frac{\partial c_A}{\partial t} = -\nabla \mathbf{J}_A. \quad (4)$$

## 3. Spinodal decomposition scenarios

The system of equations (1)–(4) was solved numerically on the 2D-region using a two-layer explicit finite-difference scheme, with non-dimensional time  $\tau = t D_A^0 / L^2$  and coordinates  $x/L, y/L$  ( $L$  is the size of the computational region). A homogeneous state with average concentration  $c_{A0}$ , with small Gaussian composition fluctuations, was chosen as the initial state. „Mirror-symmetric“ boundary conditions were used, meaning the absence of component flows through the square region boundaries.

Figures 1–4 show the results of calculations with different diffusion coefficients. Concentration levels for the component A are marked with gray gradations (the black color corresponds to  $c_A = 0$ , white — to  $c_A = 1$ ). Noticeable qualitative differences from the conventional SD kinetics (Fig. 1) occur if the  $D_A^0/D_B^0$  ratio is  $10^3 \dots 10^4$  or more (Figs. 2–4).

If the initial homogeneous state corresponds to high values of  $D(c_A)$ , composition fluctuations increase homogeneously throughout the volume, and a microstructure formed by irregularly shaped precipitates of the intermediate composition appears by the end of the wave stage of decomposition (Fig. 2). Further evolution reduces to coarsening of microstructure and removal of excessive impurity from the precipitate volume.

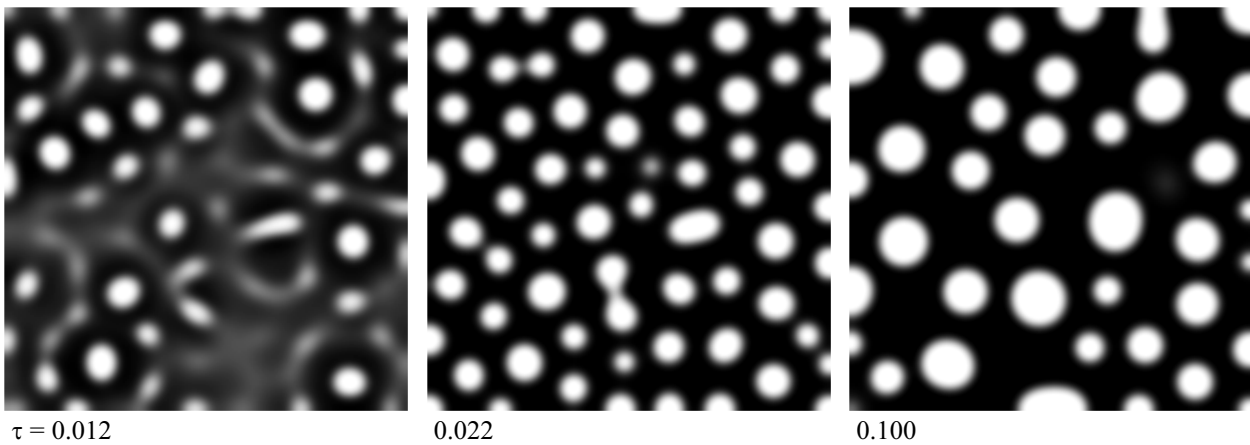


**Figure 1.** Kinetics of spinodal decomposition with  $c_{A0} = 0.3$ ,  $\Psi = 6.5$ ,  $D_A^0 = D_A^1 = D_B^0 = D_B^1$ ,  $R/L = 7 \cdot 10^{-3}$ .

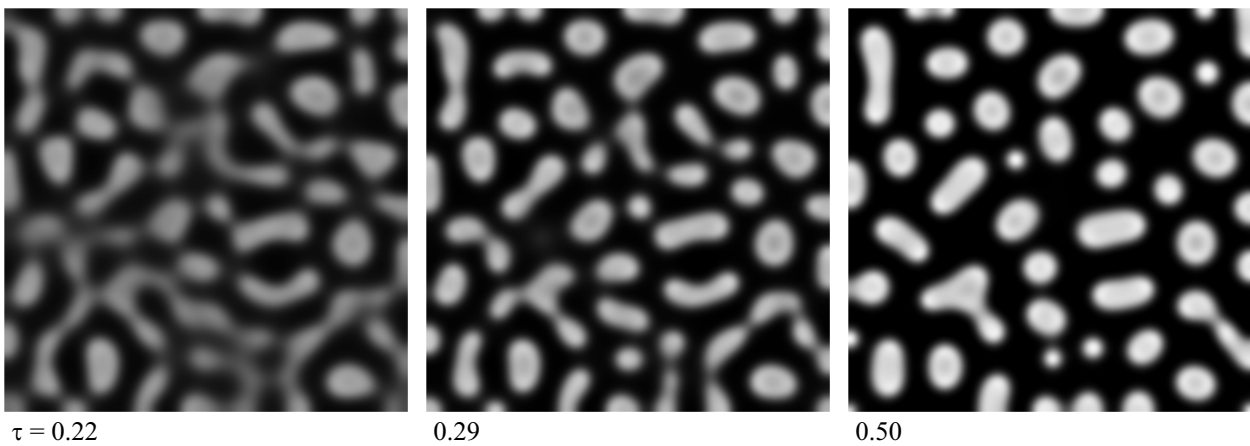


**Figure 2.** Kinetics of spinodal decomposition with  $c_{A0} = 0.3$ ,  $\Psi = 6.5$ ,  $D_A^0/D_B^0 = D_B^1/D_A^1 = 10^4$ ,  $D_A^0/D_B^1 = 1$ ,  $R/L = 7 \cdot 10^{-3}$ .

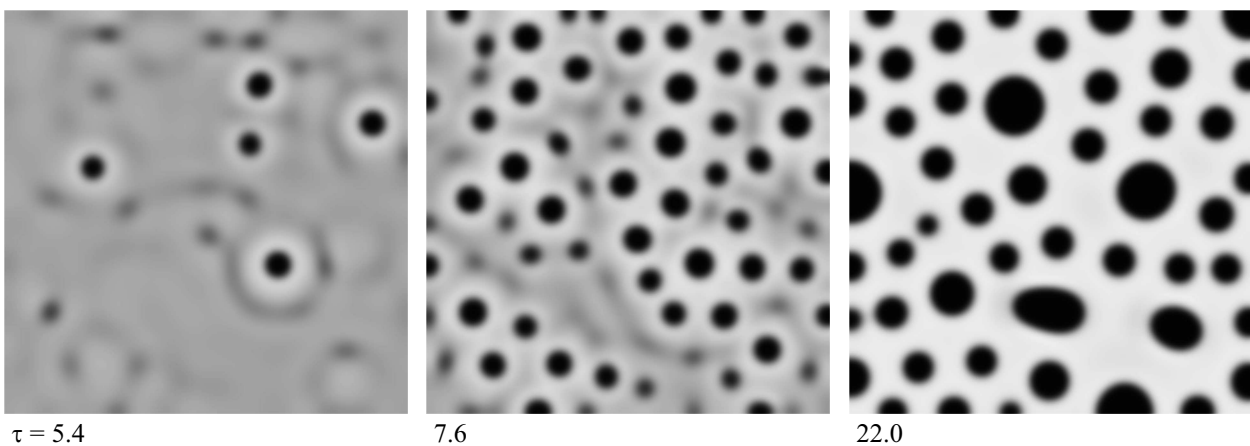


**Figure 3.** Kinetics of spinodal decomposition with  $c_{A0} = 0.7$ , the other parameters are identical to Fig. 2.

If the initial homogeneous state corresponds to low values of  $D(c_A)$ , then a dispersed structure appears after a long holding; it is formed by regularly shaped drops that have a composition close to the equilibrium one and a slightly smaller size, as compared to the structure forming in case of  $D = \text{const}$  (Fig. 3). Thereat, the base is oversaturated with

the component A even after the formation of precipitates, while the trend of autocatalysis of precipitates at the wave stage (when the formed precipitate cause new precipitates to appear in their own vicinity) is more noticeable than in the case of  $D = \text{const}$ , where the wave stage develops relatively uniformly across the volume. The drop evaporation-

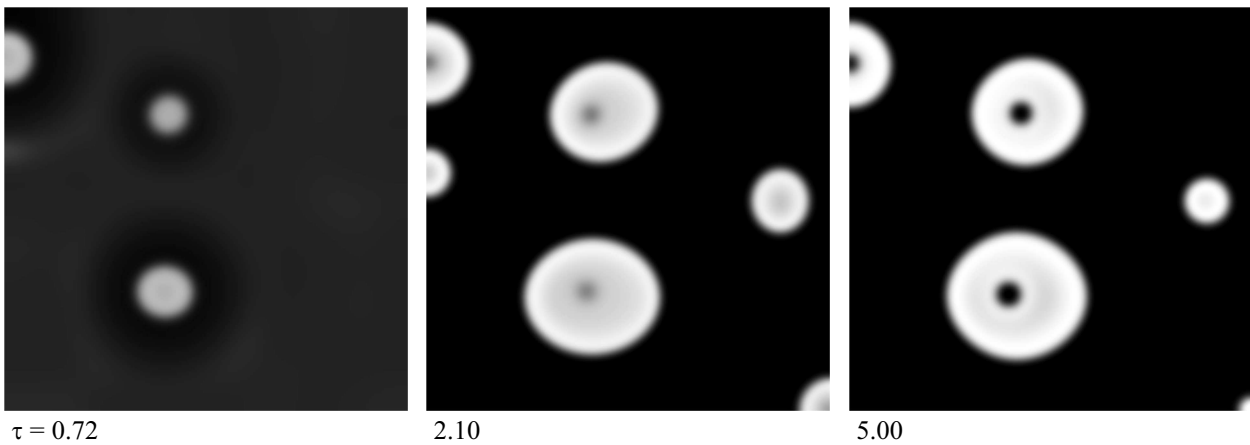


**Figure 4.** Kinetics of spinodal decomposition with  $c_{A0} = 0.2$ , the other parameters are identical to Fig. 2.

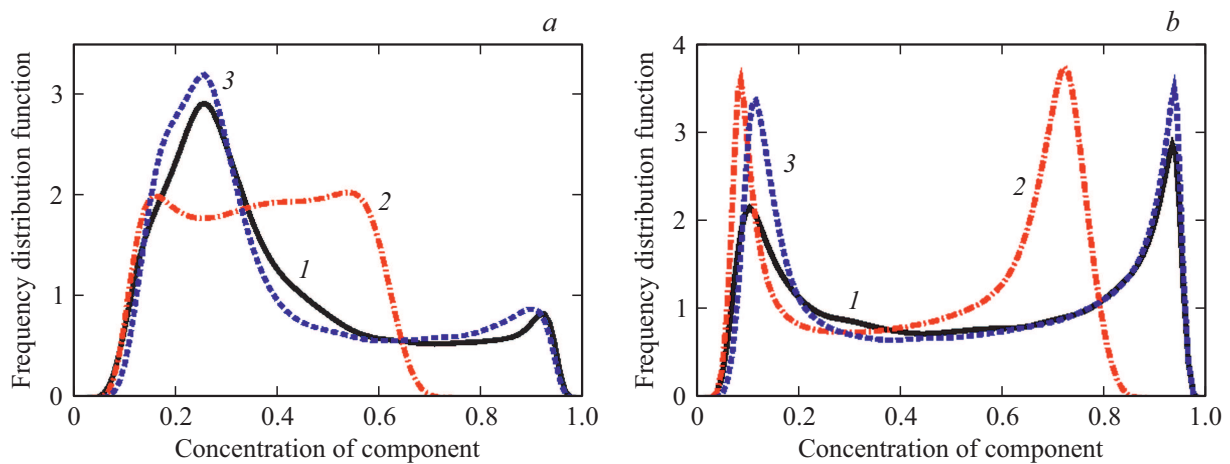


**Figure 5.** Function of distribution by concentrations of the component that forms precipitates at the parameters corresponding to Fig. 1 (curve 1), Fig. 2 (curve 2), Fig. 3 (curve 3) at the time moment corresponding to attainment of decomposition degree 0.3 (a), 0.5 (b).

condensation stage is suppressed because decomposition development is accompanied with a decrease of diffusion rate in the matrix.

When the average concentration decreases, precipitates become more rare (compare Figs. 4 and 2), so that a greater amount of impurity is trapped in their volume. This impurity does not have time to diffuse from the precipitate volume into the matrix the base even at developed decomposition stages, which eventually causes the formation of secondary precipitates into the primary ones (Fig. 4).

Decomposition kinetics can be conveniently analyzed by introducing the integral degree of decomposition

$$S_{dec} = (2c_{A0}(1 - c_{A0}))^{-1} \int |c_A(\mathbf{r}) - c_{A0}| d\mathbf{r}, \quad (5)$$

where  $c_{A0}$  is the average concentration of the component A for the specimen. Value of  $S_{dec}$  may take on values from 0 (in the homogeneous state) to 1 (in case of decomposition into pure components).

Moreover, it is convenient to introduce a function of component distribution by concentrations. The value of this function at a specified concentration corresponds to

the density of the probability that a randomly chosen atom is in a region of space with the corresponding local concentration. In the beginning of evolution, this function has one maximum that corresponds to the average component concentration. Upon decomposition completion, it has two maxima that correspond to the equilibrium solubility limits.

Figure 5 shows the charts of the function of component distribution by its concentrations upon reaching the identical decomposition degree  $S_{dec}$  in three above-mentioned kinetics scenarios (Figs. 1–3). At that, the component that forms precipitates is considered, i.e. the component A in the first two scenarios and the component B in the latter case. Presence of precipitates of the intermediate composition in the scenario shown in Fig. 2 is expressed as follows: the corresponding distribution function (curve 2 in Fig. 5) has a maximum in the region of intermediate concentrations 0.6 . . . 0.8. As distinct from this, the second maximum of the function in case of conventional SD occurs right near the equilibrium solubility limit (see curve 1 in Fig. 5). Over-saturation of the base in the scenario shown in Fig. 3 is expressed as follows: at advanced decomposition

stages, the maximum of the distribution function (curve 3 in Fig. 5) with small concentrations ( $\sim 0.1$ ) is located slightly to the right from the corresponding maxima for the other scenarios.

## 4. Discussion

It follows from the aforesaid that precipitates of intermediate composition during alloy decomposition may form most likely under low temperatures. Thereat, average component concentrations must be comparable, i.e. this means, in the first place, concentrated solid solutions. In this case, the typical diffusion length for an atom in the base is comparable to the precipitate size; at the same time, low temperature ensures a high  $D_A^0/D_B^0$  ratio, so that decomposition may take place in conditions far from local equilibrium.

Alloy decomposition at low temperatures occurs with a low speed, that's why its experimental observation is usually possible only in case of an external impact, which by itself can change the transformation kinetics. Thus, in conditions of low-temperature severe plastic deformation when diffusion rate increases by several orders, precipitates of the intermediate composition were experimentally observed in the Ag–Cu [16], Fe–Cu [17] alloys. However, the explanation in these cases deals more with effects of direct mechanical mixing [18] or with non-equilibrium diffusion transformations [19], the more so because similar disperse states in these alloys occur when processing a mixture of pure components.

The papers [20,21] gave results of 3D-atom-probe tomography that show the precipitates of BCC-copper of the intermediate composition in the BCC–Fe matrix at early decomposition stages with  $T \sim 1000$  K. However, the results of these experiments are contradictory; it appears that the effect occurs only in multicomponent alloys. Based on the table, „loose“ precipitates of iron in the copper matrix, but not vice versa, should be anticipated in the FCC-lattice. There is no data on coefficients of impurity diffusion in the volume of metastable precipitates of BCC-copper, so it is impossible to specify an assumed composition of precipitates by the end of the wave stage of decomposition in this case.

Paper [22] gives the results of 3D-atom-probe of tomography for the initial stage of spinodal decomposition in the FeCr alloy containing about 30 at.% of chromium. In this case the precipitates sized about 15 nm have a composition in the region of intermediate chromium concentrations ( $\sim 50$  at.%) and an irregular shape, which seems to qualitatively agree with Fig. 2.

## 5. Conclusion

The paper has predicted that precipitates of the intermediate composition may form (as well as secondary precipitates inside the primary ones) during spinodal decomposition

in a concentrated solid solution under a sufficiently low temperature, when impurity diffusion coefficients differ significantly.

## Funding

The work has been performed under the state assignment on topic „Structure“ No. AAAA-A18-118020190116-6.

## Conflict of interest

The author declares that he has no conflict of interest.

## References

- [1] J. Christian. *Teoriya prevrashcheniy v metallakh i splavakh*. Mir, M. (1978). 806 p. (in Russian).
- [2] J.W. Cahn, J.E. Hilliard. *J. Chem. Phys.* **28**, 258 (1958).
- [3] J.W. Cahn. *Acta Met.* **9**, 795 (1961).
- [4] J.W. Cahn. *Trans. Met. Soc. AIME* **242**, 166 (1968).
- [5] V.G. Vaks, S.V. Beiden, V.Yu. Dobretsov. *JETP Letters* **61**, 65 (1995).
- [6] V.G. Vaks. *Phys. Rep.* **391**, 3–6, 157 (2004).
- [7] I.M. Lifshits, V.V. Slyozov. *J. Phys. Chem. Solids* **19**, 35 (1961).
- [8] A.D. Smigelskas, E.O. Kirkendall. *Trans. Am. Inst. Min. (Met.) Engrs.* **171**, 130 (1947).
- [9] Ya.E. Geguzin. *Diffuzionnaya zona*. Nauka, M. (1979). 344 p. (in Russian).
- [10] V.L. Gapontsev, I.K. Razumov, Yu.N. Gornostyrev, A.E. Yermakov, V.V. Kondratyev. *PMM* **99**, 4, 26 (2005).
- [11] I.K. Razumov, Yu.N. Gornostyrev. *Vliyanie granits zeren na kinetiku raspada tverdykh rastvorov*. In: *Nauch. tr. IV shk.-seminara „Fazovye i strukturnye prevrashcheniya v stalyakh“*, Magnitogorsk (2006). P. 99–112 (in Russian).
- [12] I.K. Razumov, Yu.N. Gornostyrev, A.Ye. Yermakov. *J. Alloys Compd* **434–435**, 535 (2007).
- [13] *Protsessy vzaimnoy diffuzii v splavakh* / Ed. by K.P. Gurov. Nauka, M. (1973). 359 p. (in Russian).
- [14] S.V. Terekhov. *Technical Physics* **77**, 8, 36 (2007).
- [15] Landolt-Börnstein: *Numerical Data and Functional Relationships in Science and Technology*. New Series, Group III: *Crystal and Solid State Physics*. V. 26. *Diffusion in Metals and Alloys* / Ed. H. Mehrer. Springer-Verlag, Berlin (1990). 747 p.
- [16] F. Wu, D. Isheim, P. Bellon, D.N. Seidman. *Acta Mater.* **54**, 2605 (2006).
- [17] N. Wanderka, U. Czubayko, V. Naundorf, V.A. Ivchenko, A.Ye. Yermakov, M.A. Uimin, H. Wollenberger. *Ultramicroscopy* **89**, 189 (2001).
- [18] P. Bellon, G. Martin. *Phys. Rev. B* **39**, 4, 2403 (1989).
- [19] I.K. Razumov, Yu.N. Gornostyrev, A.E. Yermakov. *Physics of the Solid State* **61**, 2, 346 (2019).
- [20] D. Isheim, M.S. Gagliano, M.E. Fine, D.N. Seidman. *Acta Mater.* **54**, 841 (2006).
- [21] M. Schober, E. Eidenberger, P. Staron, H. Leitner. *Microsc. Microanal.* **17**, 26 (2011).
- [22] W. Xiong, P. Hedstrom, M. Selleby, J. Odqvist, M. Thuvander, Q. Chen. *CALPHAD* **35**, 355 (2011).